Energy transfer of keV Ne atoms to the lattice of a LiF(001) surface under channeling

H. Winter, A. Mertens, and R. Pfandzelter
Institut für Physik der Humboldt-Universität zu Berlin, Invalidenstraße 110, D-10115 Berlin, Germany

V. Staemmler
Lehrstuhl für Theoretische Chemie, Ruhr-Universität Bochum, Universitätsstraße 150, D-44801 Bochum, Germany
(Received 18 March 2002; published 20 August 2002)

The energy loss of neutral Ne atoms with keV energies scattered under a glancing angle of incidence from a flat LiF(001) surface is investigated by means of a time-of-flight method. Under these scattering conditions, i.e., surface channeling, electronic excitations of the insulator surface as well as charge-exchange processes play a negligible role, so that the elastic energy transfer of projectiles to atoms of the target surface can be studied. Our data are interpreted by Monte Carlo computer simulations based on quantum-chemical interaction potentials. The simulations show that thermal vibrations of lattice atoms play an important role for a quantitative description of projectile energy loss under channeling. From our simulations we derive a surface Debye temperature of 250 ± 50 K for the LiF(001) surface.

DOI: 10.1103/PhysRevA.66.022902 PACS number(s): 79.20.Ap, 34.50.Bw, 34.50.Dy, 68.35.Ja

I. INTRODUCTION

The dissipation of kinetic energy of atomic projectiles in matter proceeds in terms of electronic excitations (''electronic stopping'') and elastic collisions with target atoms (''nuclear stopping''). The latter mechanism contributes only at low projectile velocities, i.e., $v < v_0$ (v_0 denotes Bohr velocity) and dominates the angular deflection of projectiles in the scattering event [1]. A particular regime of ion-solid interactions is achieved under ''channeling,'' where the projectiles collide with atoms of a crystal in a sequence of correlated small-angle scattering events [2–8]. This condition is met for projectile impact close to a low index axis or plane of the crystal lattice and results in well defined projectile trajectories characterized by relatively large impact parameters. It is simple to show (see also below) that, for collisions in the channeling regime, the transfer of projectile energy to target atoms of the crystal lattice is very small in comparison to electronic dissipation processes. As a consequence, electronic stopping phenomena in solids can then be studied fairly well even at low projectile velocities [9–14].

Until recently, it was a well-known fact that under channeling the contributions of an energy transfer of projectiles to atoms of the crystal are ''negligibly'' small, however, no specific information was available on the actual size of this process. This status can simply be explained by the dominance of electronic processes under these conditions of scattering, i.e., single and collective excitations of target electrons, response phenomena, and charge exchange. As a consequence, a specific feature of channeling could not be explored in previous experimental studies. Ritchie and Manson [15] investigated this problem theoretically and concluded a surprisingly large transfer of projectile energy to the crystal lattice, which was termed ''mechanical energy loss'' by the authors. These calculations were performed for scattering of projectiles from a crystal surface under a grazing angle of incidence so that conditions of ''surface channeling'' are fulfilled and projectiles are reflected from the solid in front of the topmost layer of surface atoms and do not penetrate into the bulk of the solid. This regime of ion surface scattering is characterized by the general features of channeling [4–7], which have been exploited in recent years to study stopping phenomena of ions in the electron selvedge of metal surfaces. In those studies detailed information on electronic stopping mechanisms has been revealed [11–14] by assuming that nuclear stopping contributes to the overall dissipation of projectile energy in a negligible manner.

Recently, we reported on experiments of scattering keV Ne atoms from a flat and clean LiF(001) surface under a grazing angle of incidence [16]. Owing to specific features of charge exchange of atoms and ions in front of wide-band-gap insulators, i.e., suppression of charge exchange via resonant electron transfer or Auger-electron neutralization, this channel for inelastic projectile energy loss can be ruled out. Then excitations of lattice atoms via long-ranged Coulomb interactions (''optical phonons'' [17]) play a dominant role for stopping of ions in front of insulator surfaces [18,19]. It turns out that this contribution to stopping can be avoided also by making use of neutral atoms as primary projectiles. As a consequence, the elastic energy transfer from projectiles to lattice atoms is the dominant mechanism for energy loss under these conditions, and nuclear stopping under channeling conditions could be studied [16,20].

In this paper we will present details on experimental and theoretical descriptions of this interesting phenomenon in the field of ion-solid interactions. We will first present some simple estimates on the elastic energy transfer of atomic projectiles to a crystal lattice for scattering from a string or plane of atoms in the regime of channeling. Then we outline in detail our experimental setup that comprises of a high-resolution time-of-flight (TOF) device for measurements on energy loss of neutral Ne atoms with keV energies from a LiF(001) surface. We discuss the evaluation and correction of data, since the variation of the path length for different angles of scattering and its effect on the flight time is of pivotal importance for the measurements. Our data are interpreted by means of Monte Carlo computer simulations. These calculations reveal that the energy transfer from

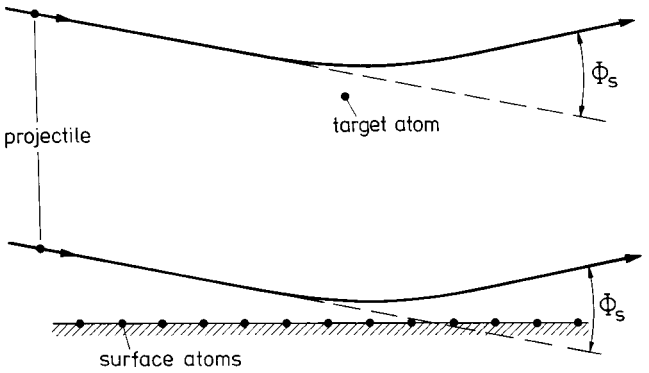

FIG. 1. Sketch in order to illustrate scattering of atomic projectiles from a single target atom by angle Φ_s and from a string of target atoms representing the topmost layer of a surface.

atomic projectiles to atoms of the topmost layer of the crystal lattice is affected in a decisive manner by thermal vibrations of lattice atoms. By making use of atomic interaction potentials obtained from calculations, we derive the surface Debye temperature of LiF(001) from best fits of our simulations to the experimental data.

II. SIMPLE ESTIMATES ON ELASTIC ENERGY TRANSFER IN ATOMIC COLLISIONS

We begin our discussion on the intricate problem on nuclear stopping for ion-solid interactions under channeling conditions with simple estimates based on classical mechanics and conservation of energy and momentum. For the general case, we obtain for the energy E_1 of projectiles with incident energy E_0 and mass M_1 after elastic scattering from a single target atom with mass M_2 under an angle Φ_s as sketched in the upper panel of Fig. 1 [5,21],

$$E_1 = E_0(\cos\Phi_s + \sqrt{(M_2/M_1)^2 - \sin^2\Phi_s})^2/(1+M_2/M_1)^2. \tag{1}$$

For angular deflections, $\Phi_s < 2°$, typical for low-energy channeling from surfaces, one obtains from Eq. (1) for $M_1 \approx M_2$ an energy transfer to the target atom (energy loss for projectiles) $\Delta E_1 = E_0 - E_1 < 10^{-3} E_0$ in a single binary encounter. For a steering of projectiles by a string (or plane) of atoms as illustrated in the lower panel of Fig. 1, the total scattering angle Φ_s is the result of a collision sequence with angular deflections $\Phi_i \ll \Phi_s$ and $\Phi_s = \Sigma_i^n \Phi_i$. In the regime of small angles, Eq. (1) can be written as

$$\Delta E_1 \approx E_0 \frac{M_1}{M_2} \sin^2\Phi_s \approx E_0 \frac{M_1}{M_2} \Phi_s^2. \tag{2}$$

Assuming, for simplicity, that Φ_s results from a number of n comparable deflections Φ_i, i.e., $\Phi_s = n\Phi_i$, we have

$$\Delta E_n = \sum_1^n \Delta E_i \approx n E_0 \frac{M_1}{M_2} \left(\frac{\Phi_s}{n}\right)^2 = \Delta E_1 / n, \tag{3}$$

so that the energy loss ΔE is reduced by about the number n of effective collisions with lattice atoms. E.g., for $n = 10$ we have $\Delta E_n = \Delta E_1/10 < 10^{-4} E_0$ in the specific case mentioned. This is indeed a very small fraction of energy dissipated to the crystal lattice. It is interesting to note that the small energy loss in small-angle scattering of projectiles with atoms in the gas phase is further reduced by the number of effective collisions n. As a consequence, nuclear stopping can be considered as being negligible in view of electronic processes effective under atomic collisions with solids under channeling. This feature has been made use of in a fair number of studies, in particular with low-energy ions, in order to investigate features of electronic stopping phenomena in solids and at surfaces [9–14]. In those studies, the nuclear energy loss was generally considered as being negligibly small, but its actual magnitude was never discussed nor derived from an experiment so far.

In the following, we describe first our experimental setup and procedures and then computer simulations on the scattering of keV neutral Ne atoms from a clean and flat LiF(001) surface under a glancing angle of incidence. These studies allow us to derive detailed data and information on the projectile energy transfer to the crystal lattice in this regime of scattering.

III. EXPERIMENT

In our experiments, we performed TOF studies in order to measure the energy loss of neutral Ne atoms with energies in the keV domain after grazing scattering from the surface of a LiF(001) crystal. For this collision system we could show that contributions for electronic excitations and long-range response phenomena can be ruled out [16]. Detailed studies on the elastic energy transfer to the lattice atoms can then be performed because of the following:

(1) For scattering under surface channeling conditions, processes between atomic planes within the bulk of a solid can be excluded. In particular, transmission channeling experiments can only be performed with relatively thick monocrystalline foils resulting in multiple reflections from atomic planes, whereas for surface scattering a trajectory for a single specular reflection event is effective.

(2) For a wide-band-gap material (LiF here), electronic excitations of valence electrons are strongly suppressed for low-energy ion bombardment. Furthermore, contributions of charge exchange, in particular ionization of neutral projectiles, are negligible at low projectile velocities [22].

(3) For neutral noble gas atoms no long-range Coulomb forces are relevant. These forces, present for ions, can lead to excitations of transverse-optical phonons that result for Ne^+ ions of a few keV to energy losses of some 10 eV [18,19], clearly beyond the estimated size of nuclear stopping. Choosing low-energy neutral projectiles accompanied by negligible projectile ionization during the collision eliminates this contribution to dissipation of energy completely.

The experimental setup for our TOF studies is sketched in Fig. 2. An important prerequisite for our investigations is an overall time/energy resolution in the subpermille domain, i.e., an overall energy resolution typically in eV at keV projectile energies. Ne^+ ions are produced in a hollow cathode

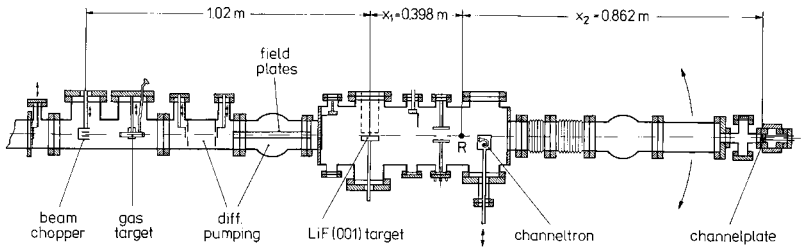

FIG. 2. Experimental setup. Note that the channel plate detector is rotated with respect to axis labeled "*R*."

ion source (SO55, High Voltage Engineering Europe, Amersfort, NL) with an energy spread of less than 1 eV [23] and are accelerated to the final projectile energy of a few keV by using a high-voltage supply with a low-ac ripple ($<$0.1 V). After deflection by a small magnet the ion beam passes through first sets of defining slits and a pair of electric-field plates for chopping the beam by fast voltage pulses with rise times smaller than 10 ns from negative to positive offset voltages. Slits and field plates are adjusted in a way that packets of ions pass this chopper unit only for voltages close to zero, resulting in effective chopping times of typically 1 ns.

The ions pass a gas target operated with Ne atoms at a pressure of about 10^{-4} mbar, where the projectiles are efficiently neutralized by resonant charge transfer with a negligible increase in energy spread for the fast atomic beam. This beam passes further slit systems (0.2-mm aperture) which are components of two differential pumping stages. The LiF(001) target was cleaved under air and mechanically polished in order to reduce the step densities of the surface. The damage introduced by the polishing procedure is removed by lengthy preparation cycles of grazing sputtering of the surface with 25-keV Ar^+ ions under an angle of incidence of about 2.5°. During sputtering the target is kept at an elevated temperature of about 300 °C where LiF shows sufficient conductivity in order to avoid a macroscopic charging up of the target sample [24]. For annealing of the surface, the temperature is raised to 400 °C for about 15 min. After a major number of cycles a clean and flat surface, widely free from defects, is obtained. The "quality" of the surface can be checked in a straightforward manner by recording angular distributions for scattered projectiles [25–27]; we observe well defined angular distributions as presented below. The target surface is kept at a base pressure of about 5×10^{-11} mbar and a temperature of 300 °C, the angle of incidence Φ_{in} is chosen from 0.5° to 2°. The flight time for specularly reflected projectiles, i.e., same angle of incidence and angle of exit, $\Phi_{in}=\Phi_{out}$, is recorded by a multichannel-plate detector behind the target. This detector can be rotated within the plane of scattering (plane contains surface normal and direction of incoming beam) with a radius of $x_2=0.862$ m with respect to an axis labeled R (see figure) which is located at a distance $x_1=0.398$ m from the target. Since this reference of rotation does not coincide with the position of the target, the effective distance between target and multichannel-plate detector varies slightly with the angle of scattering Φ_s. It turns out that this reduction of the path length with angle has a comparable effect on the data as the estimated energy loss, so that a reliable correction of this feature for the TOF spectra is crucial for the experiment and its interpretation.

For finite angles of scattering Φ_s the reduction in path length from target to detector, Δx, can be derived from simple geometrical concepts,

$$\Delta x = x_1 + x_2 - x_1 \cos\Phi_S - \sqrt{x_2^2 - x_1^2 \sin^2\Phi_S}. \qquad (4)$$

This reduction in path length leads to a smaller flight time of projectiles and thus to an enhancement of measured projectile energies

$$\Delta E = \frac{2\Delta x}{x_1 + x_2} E. \qquad (5)$$

This shift in energy is slightly lower, but still of the same order of magnitude than the elastic energy transfer to lattice atoms.

Because of the relevance of this correction for our data, we performed an additional experiment with our setup to study the effect of a modified path length as function of the angle of scattering. We slightly deflected a Ne^+ beam by a bias voltage in the target region, where the target surface is slightly translated off its position for scattering experiments. The grid of an electron detector (not operated during these studies) serves as second electrode here. A sketch of relevant components for this investigation is shown in Fig. 3. The incoming ion beam is deflected by the electric field owing to a bias voltage applied to target or grid. With a voltage of up to 100 V, the beam is deflected by angles that are also achieved in the surface scattering experiments. The concept of this study is based on comparable trajectory lengths from target to detector for projectiles deflected by the electric field

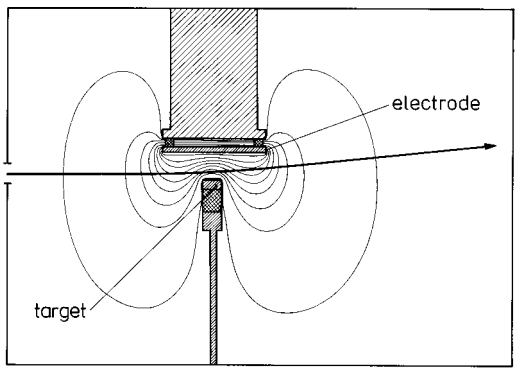

FIG. 3. Geometry in the vicinity of target and equipotential curves as calculated with SIMION.

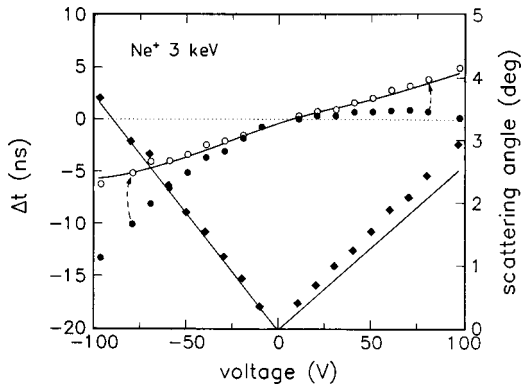

FIG. 4. Angle of scattering (full diamonds, right ordinate) and time shift (full circles, left ordinate) for 3-keV Ne^+ ions. Open circles represent data after correction for reduced path length, solid curves are the angular deflection and the time shift calculated from the potentials in the target region by SIMION.

and by scattering from the target surface. The equipotential curves drawn in the figure are calculated with the program SIMION [28].

Results from these studies are presented in Fig. 4. For positive voltages the target is biased and the grid is grounded and for negative voltages and vice versa. The full diamonds represent measured scattering angle for 3-keV Ne^+ ions as function of voltage, which agree fairly well with angular deflections computed with SIMION (solid curve). Main issue of this investigation is the effect of the angular deflection on the TOF spectra. The full circles represent measured shifts in flight time of 3-keV Ne^+ ions as function of bias voltage and also of deflection angle. This flight time is shifted by the reduced path length with increasing angle (see above), but also by the potential in the target region. The solid curve indicates the shift in flight time calculated from the potentials derived with SIMION. These data clearly deviate from the measurements. However, corrections of the flight times based on the simple geometrical approach given in Eqs. (4) and (5) provide data (open circles) that show perfect agreement within the uncertainties of the experiment. This result shows that our data can reliably be corrected with respect to the change in path length caused by a variation of the angle of scattering. In order to provide a quantitative judgement on this correction, we mention that, e.g., for 3-keV Ne atoms the shifts in path lengths and flight times result in shifts of projectile energy of $\Delta E = 0.4$ eV at a scattering angle of $\Phi_s = 1°$, 1.7 eV at 2°, and 3.8 eV at 3°.

IV. EXPERIMENTAL RESULTS

After careful preparation of the LiF(001) surface, well defined angular distributions for scattered projectiles serve as an indication for a clean and flat target, widely free from defects [26,27]. As an example, we show in Fig. 5 two angular distributions for $\Phi_{in} = 1°$ (left panel) and $\Phi_{in} = 2°$ (right panel) recorded by translation of a channeltron detector within the plane of scattering at a distance of 0.45 m behind the target. A reference for the direction of the incoming beam is derived from the intense signal owing to the

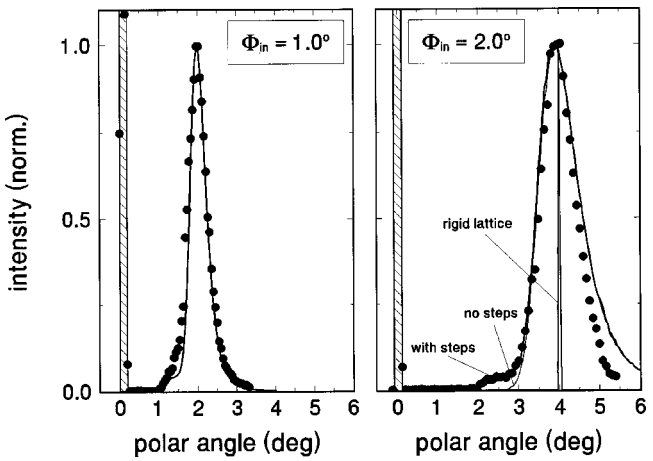

FIG. 5. Angular distributions for 3-keV N atoms scattered from the LiF(001) surface under $\Phi_{in} = 1°$ (left panel) and $\Phi_{in} = 2°$ (right panel). Solid curves represent results from computer simulations as outlined in text.

residual fraction of the well-collimated projectile beam that does not hit the target and has passed above the surface without scattering (peak at the left side of the distribution). The angular distributions for scattered atoms show a pronounced and defined peak at the direction of specular reflection, i.e., $\Phi_{in} = \Phi_{out} = \Phi_s/2$. The solid curves represent results from computer simulations discussed below.

In Fig. 6 we display representative energy spectra for 3-keV Ne atoms scattered from the LiF(001) surface under specular reflection, where the TOF spectra have been transformed to an energy scale and corrected with respect to the effective path length (see discussion in preceding section). The open circles in the figure represent an energy spectrum recorded for the projectile beam where the target has been taken out of the beam axis so that the atoms reach the channel-plate detector without scattering from the surface. The solid curves are best fits to Gaussian line shapes that describe

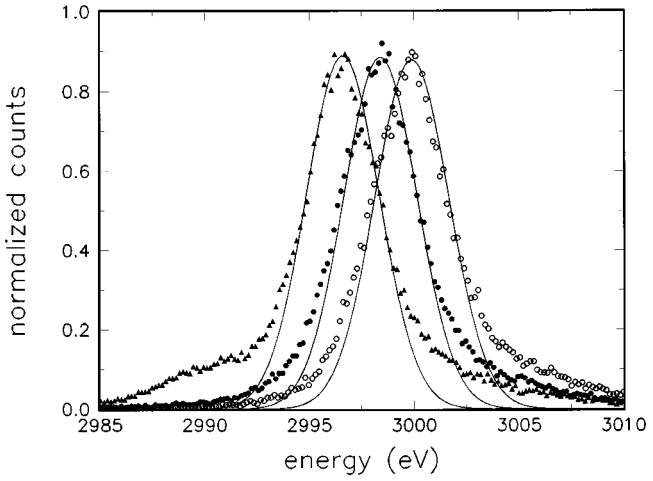

FIG. 6. TOF spectra (converted to energy scale) for 3-keV Ne atoms scattered from the LiF(001) surface under specular reflection. Open circles, direct beam; full circles, angle of incidence $\Phi_{in} = 1.05°$; full triangles, $\Phi_{in} = 1.75°$.

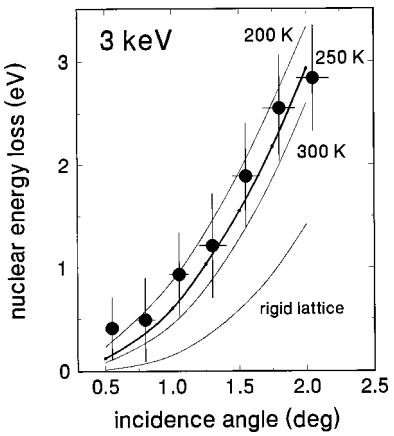

FIG. 7. Nuclear energy loss as a function of angle of incidence for 3-keV Ne atoms scattered from the LiF(001) surface. The solid curves represent results from computer simulations using surface Debye temperatures of 200, 250, and 300 K as well as rigid lattice.

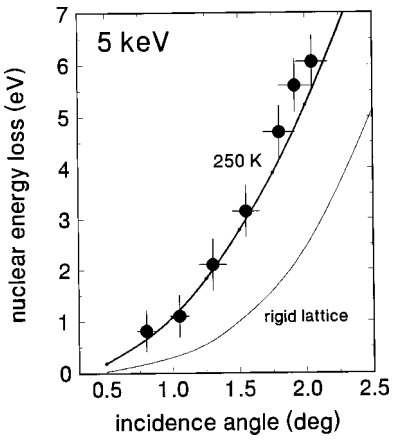

FIG. 8. Nuclear energy loss as a function of angle of incidence for 5-keV Ne atoms scattered from the LiF(001) surface. The solid curves represent results from computer simulations using a surface Debye temperature of 250 K as well as rigid lattice.

the central part of the peaks fairly well. The spectrum for the incident beam has a full width at half maximum of about 3.5 eV, i.e., the overall energy spread of our setup amounts to typically 10^{-3}. Closer inspection of the peaks reveals wings at the low- and high-energy sides, which we attribute to effects caused by the timing of our chopping unit and by change of energy owing to charge exchange of the incident ions in the gas target. These wings in the spectra, however, will be neglected here, since we concentrate on the most probable energy loss given by the well defined maxima of the peaks.

The full circles represent a spectrum obtained for projectiles scattered from the LiF surface under an angle of incidence $\Phi_{in}=1.05°$, which shows a shift of 1 eV in comparison to the incident beam. These data demonstrate that the overall energy resolution of our setup is sufficiently high to resolve such a small energy loss of only about 10^{-4}. For $\Phi_{in}=1.75°$ (full triangles) the data show a further slight increase of the energy loss. Note that in the low-energy tail of the spectrum a broader structure can be identified for larger impact angles and energies. In the studies presented here we have not investigated this feature in more detail, because this part of the spectrum does not affect the prominent peak structure owing to elastic energy transfer. The origin of this part of the energy spectrum is ascribed to electronic processes, primarily excitations of the target [29,30], where energy losses of less than about 10 eV might be attributed to excitations of the projectile atoms.

Most probable energy losses are derived from spectra as shown and plotted as function of angle of incidence in Fig. 7 for 3 keV and in Fig. 8 for 5 keV Ne atoms. The observed monotonic increase of the energy loss with angle is similar for the two energies, where the energy loss at the larger projectile energy is systematically higher. The solid curves in both figures represent the analysis of data based on classical trajectory Monte Carlo simulations as outlined in the following section. The data displayed here are to the best of our knowledge the first measurements on the elastic energy transfer to a crystal lattice under channeling conditions. Our measurements show that this mechanism for projectile energy loss is, as expected, clearly smaller than electronic processes. In the following we will discuss the analysis of our data and reveal some interesting features on stopping in this regime. We will show that thermal vibrations of lattice atoms play an essential role for an understanding of nuclear stopping of channelled atomic projectiles.

V. EVALUATION OF DATA AND DISCUSSION

The data presented in the preceding section are analyzed in terms of Monte Carlo computer simulations in order to handle the complex many-body problem. Essential aspects on these simulations have been outlined in a recent paper [20], however, for the studies presented here we have chosen atomic interaction potentials for Ne atoms in front of a LiF(001) surface that are derived from quantum-chemical *ab initio* methods. It turns out that in particular the long-range behavior of those individual quantum-chemical potentials is substantially different from pair potentials obtained in the Thomas-Fermi approach with corresponding screening functions [1,31]. Our quantum-chemical calculations are based on a LiF(001) surface represented by a $(LiF_5Li_{13})^{9+}$ cluster containing one central Li^+ ion with five F^- ions directly coordinated to it and 13 Li^+ cations in the next coordination shell. This cluster is embedded in an extended point-charge field of $27\times27\times6=4374$ point charges with ionicities ±1. In order to speed up the convergence of the Madelung energy, fractional charges were placed at the outermost borders of the point-charge array, as proposed by Evjen [32]. The complete system, i.e., cluster plus point-charge field, is charge neutral. The lattice constant $a=4.0262$ Å of the undistorted LiF crystal [33] was used both for the cluster and the point-charge field; no relaxations of the (001) surface were considered.

The full interaction potential was calculated in the form of potential-energy curves for Ne atoms in front of the LiF(001) surface at different positions: Li ontop site (Li), F ontop site (F), midpoint between two F (or Li) atoms (*M*). The distance of Ne atoms from the topmost surface layer was varied be-

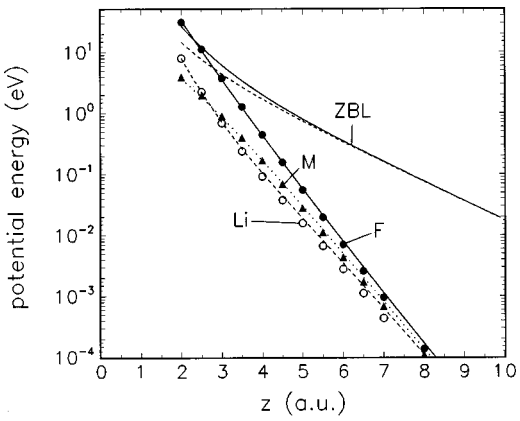

FIG. 9. Potential energy for interaction of a Ne atom with LiF(001) surface ($z=0$ is referred to the topmost layer). ZBL represents the potential for universal screening, symbols represent results from quantum-chemical calculations (full circles represent on top of F^- ions, open circles represent on top of Li^+ ions, and full triangles are for ''middle position''). For details see text.

tween 2 and 10 a.u.; beyond 10 a.u. the interaction energies are negligibly small. All calculations were performed at the Hartree-Fock level. This approximation yields the predominant contribution to the interaction between closed-shell systems such as Ne and the LiF(001) surface, in particular, in the range of intermediate and large interaction energies. Van der Waals interactions (London dispersion forces) cannot be described in this way, so that the physisorption of Ne on LiF(001) is not included in these calculations. In view of the fast motion of the Ne atoms we estimate the uncertainties for our static description, which amount to the same order of magnitude as physisorption potentials. Reasonably large Gaussian basis sets of quadruple zeta quality with several sets of polarization functions are used. The *sp* parts of the basis sets for Li and F were taken from Ref. [34], for Ne from Ref. [35]. Since these basis sets are rather large, the basis set superposition errors turned out to be small; nevertheless, all results were corrected by means of the full counterpoise method of Boys and Bernardi [36].

In Fig. 9 we have plotted the calculated potential energies for a Ne atom in front of a LiF(001) surface as function of distance z from the topmost surface layer. The full circles represent calculations for a position on top of a F^- site (labeled F), the open circles on top of a Li^+ site (Li), and the full triangles for a position in the middle of a unit cell (M). The data reveal a functional dependence on z close to a single exponent decay. Comparison with the potential, commonly used for fast atomic collisions with solids, proposed by Ziegler, Biersack, and Littmark (''ZBL potential'' [1]),

$$V(r)=\frac{Z_1Z_2}{r}\sum_i a_i \exp(-b_i r/a_u), \tag{6}$$

with $a_i=\{0.1818,0.5099,0.2802,0.028\,17\}$ and $b_i=\{3.2,0.9423,0.4028,0.2016\}$ being constants for ZBL screening and

$$a_u=\frac{0.8553\ \text{a.u.}}{(Z_1^{0.23}+Z_2^{0.23})} \tag{7}$$

is the universal screening length [1], shows that the universal potential is comparable at the smallest distances relevant for our studies. However, at larger distances we find a significant stronger repulsive potential for the ZBL approach than derived from the quantum-chemical code.

For the computer simulations outlined below the interatomic potentials are of paramount importance, since trajectories of scattered projectiles are computed from these potentials. In comparison to our recent studies [20], we have modified the simulations on trajectories during atom surface scattering by making use of quantum-chemical potentials. These potentials are incorporated in the available program by the approximation of a Bohr type of screening, i.e., pair potentials for Ne-Li^+ and Ne-F^- are given by exponential screening,

$$V(r)=\frac{Z_1Z_2}{r}\exp(-c_{12}r/a_u). \tag{8}$$

The constants c_{12} are derived from correlated best fits to the three data sets shown in Fig. 9 (curves drawn through data in figure). The data are well described by this simple approximation with $c_{12}=0.622$ for Ne-Li^+ and $c_{12}=0.481$ for Ne-F^-. Based on these potentials, trajectories for Ne atoms scattered under grazing incidence from a LiF(001) surface are derived in the framework of classical mechanics by assuming a sequence of elastic binary collisions of neutral Ne atoms with Li^+ and F^- ions imbedded at lattice sites of a semi-infinite crystal. As pointed out, electronic processes, such as electron-hole pair and plasmon excitation, as well as charge transfer, electronic promotion, and long-ranged excitation of transverse-optical phonons can be neglected for the specific system investigated here. In accordance with the experiments a ''random'' azimuthal orientation of the target surface was chosen by an azimuthal angle a few degrees off the [100] direction in the plane of the crystal surface. The simulations were performed with a DEC 3000-600 workstation, and typically 10^6 trajectories of scattered projectiles are followed and analyzed with respect to angular scattering and final energies.

In detailed studies on angular distributions for keV ions scattered under grazing incidence from metal surfaces it was revealed that the defect structure of the target surface and thermal vibrations of lattice atoms are essential to describe the experiments on a quantitative level [27]. A slight miscut of the crystal with respect to a defined crystallographic plane results, for a smooth surface, in terraces formed by topmost layer atoms separated by steps. In the simulations this feature is incorporated by flat terraces of geometrically distributed lengths separated by steps of monoatomic height with ''upward'' or ''downward'' orientation. Quantitative low-energy electron diffraction studies suggest a shift of the subplane of Li^+ cations by 0.25 Å towards the bulk with respect to the subplane of F^- anions [37]. Such a ''rumpling'' seems to be a general feature of alkali halides owing to the different ionic radii [38]. This finding, however, was questioned by experi-

ments on scattering of thermal He atoms [39] and atomic force microscopy [40], where only a small and opposite rumpling by about 0.036 Å was deduced. Since the question on the equilibrium structure of the LiF(001) surface is not settled [41], we have also investigated the effect of surface rumpling on the data.

Thermal vibrations of lattice atoms modify the distance between projectiles and target atoms and affect the scattering process in a decisive manner. The effect of thermal vibrations on projectile trajectories manifests itself in the width of angular distributions for scattered particles. Computer simulations have shown that for a surface of good quality the angular width is primarily determined by those vibrations [27]. In our simulations, uncorrelated thermal vibrations of surface atoms perpendicular to the surface plane are taken into account in using the harmonic model with a Gaussian probability density function for the elongation of lattice atoms [42]. From the Debye model in high-temperature approximation we obtain mean-square displacements of atom [43],

$$\langle u_{\perp}^2 \rangle = 3\hbar^2 T / M_2 k_B \theta_{D\perp}^2, \tag{9}$$

with M_2 being the mass of lattice atoms (Li or F) and $\Theta_{D\perp}$ the surface Debye temperature. In accordance with the experiments, a temperature of the target surface of $T=573$ K is chosen. Since the velocities of projectiles exceed those of the vibrating lattice by about three orders of magnitude, a ''frozen lattice'' can be considered for individual binary collisions. The elastic energy transfer is calculated using Eq. (1) from actual angular deflections in close encounters with target atoms. Summation of individual energy transfers over complete trajectories results in the total elastic transfer to the crystal lattice or nuclear energy loss for scattered projectiles.

The solid curves in Fig. 5 represent the angular distributions obtained by our computer simulations. In this respect, it is important to note that our simulations provide a consistent description of angular scattering as well as energy loss by the same set of free parameters. The angular distributions are calculated for the experimental parameters (3 keV, $\Phi_{\text{in}} = 1.0°$ and 2.0°, respectively) and terraces with geometrically distributed lengths. The structure in the foot of the peaked distribution can be used as a measure for the density of downward steps [27] and fixes this parameter with sufficient accuracy (mean distance 2000 Å here). A surface Debye temperature of $\Theta_{D\perp} = 250$ K provides a good description of the angular width of both distributions. The sensitivity of data for a specific variation of these parameters will be outlined in the following for the data on projectile energy loss.

The thick solid curves in Figs. 7 and 8 represent the results of our computer simulations for the projectile energy loss with the same set of parameters as used for the description of the angular distributions. The data represent the most probable energy loss obtained from the simulated energy spectra after convolution with the experimental energy resolution. The fair description of the experimental data by the simulations at both energies, 3 and 5 keV, may serve as an indication for the overall consistency of our analysis. Of particular interest is the sensitivity of the data on variations of the relevant parameters for the characterization of the target surface. In Fig. 7 we demonstrate the dependence of the energy loss for 3-keV projectiles on the Debye temperature by adding results for $\Theta_{D\perp} = 200$ K and $\Theta_{D\perp} = 300$ K, which differ considerably from the simulations for $\Theta_{D\perp} = 250$ K and the experimental data. These results serve to estimate the uncertainty for the surface Debye temperature derived from our data. We also have plotted in the Figs. 7 and 8 results obtained under the assumption of a rigid lattice, which substantially deviate from the experiments. This result leads us to the important conclusion that the energy transfer can only be described on a quantitative level, if thermal vibrations of lattice atoms are taken into account.

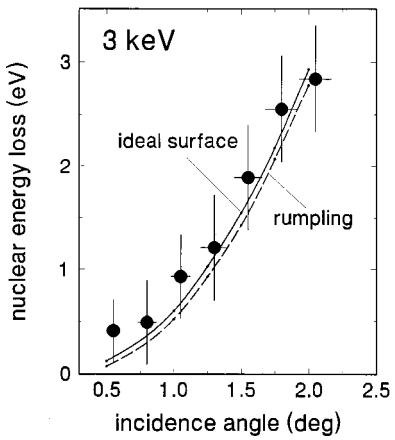

FIG. 10. Nuclear energy loss as a function of the angle of incidence for 3-keV Ne atoms scattered from the LiF(001) surface. The solid curve represents results from computer simulations for the surface Debye temperature of 250 K and ideal surface, and the dashed curve represents simulations that include surface rumpling as detailed in text.

In Fig. 10 we have investigated the effect of surface rumpling on the energy loss for 3-keV projectiles. By making use of the quantum-chemical potentials we come to the same conclusion as presented recently [20]. The effect of rumpling is small in comparison to data for an ideal surface (cf. dashed and solid curves in Fig. 10) and is equivalent to an enhancement of the Debye temperature of some 10 K only. This is below the uncertainty for $\Theta_{D\perp}$ derived from our data on energy loss.

VI. CONCLUSION

In conclusion, by making use of specific features for the scattering of fast neutral Ne atoms from the surface of a wide-band-gap insulator we have investigated in detail the energy transfer to the crystal lattice under channeling conditions. Since all mechanisms giving rise to electronic excitations or charge exchange between projectile and crystal are negligibly small here, the so-called nuclear energy loss can be studied on a quantitative level. Our data are analyzed in terms of Monte Carlo computer simulations based on classical mechanics where projectile trajectories are calculated by using quantum-chemical interatomic potentials between Ne atoms and Li^+ or F^- ions imbedded in the crystal. The computer simulations reveal clearly that thermal vibrations of

lattice atoms play a dominant role for a quantitative description of the experimental data. Angular distributions and the energy loss of scattered particles can consistently be described in our computer simulations by the same set of parameters characterizing the target surface. The lattice vibrations are described within the framework of the Debye model by the surface Debye temperature that is deduced here in a conservative estimate to $\Theta_{D\perp} = 250 \pm 50$ K. This temperature is considerably smaller than the bulk Debye temperature of 732 K. Surface Debye temperatures derived from diffraction patterns for thermal H and He atom scattering yield after elaborate corrections $\Theta_{D\perp} = 415 \pm 40$ K [44] and $\Theta_{D\perp} = 350 \pm 50$ K [45,46]. These values are somewhat higher than the Debye temperature derived from our scattering experiments. In view of the present status of the different experiments and their analysis it is not possible to clear up the slight deviations found in the conclusions on $\Theta_{D\perp}$.

ACKNOWLEDGMENT

This work was supported by the Deutsche Forschungsgemeinschaft under Contract No. Wi 1336.

[1] J. F. Ziegler, J. P. Biersack, and U. Littmark, *The Stopping and Range of Ions in Solids* (Pergamon, New York, 1985).
[2] M. T. Robinson and O. S. Oen, Phys. Rev. **132**, 2385 (1963).
[3] J. A. Davies, Phys. Scr. **28**, 294 (1983).
[4] D. S. Gemmell, Rev. Mod. Phys. **46**, 129 (1974).
[5] L. C. Feldman and J. W. Mayer, *Fundamentals of Surface and Thin Film Analysis* (Elsevier, Amsterdam, 1986).
[6] M. W. Thompson, in *Channeling*, edited by D. W. Morgan (Wiley, New York, 1973), p. 1.
[7] R. Sizmann and C. Varelas, Festkoerperprobleme **17**, 261 (1977).
[8] H. F. Krause and S. Datz, Adv. At., Mol., Opt. Phys. **37**, 139 (1996).
[9] J. H. Omrod, J. R. MacDonald, and H. E. Duckworth, Can. J. Phys. **43**, 275 (1965).
[10] D. Ward, H. R. Andrews, I. V. Mitchell, W. N. Lennard, R. E. Walker, and N. Rud, Can. J. Phys. **57**, 645 (1979).
[11] K. Kimura, M. Hasegawa, and M. Mannami, Phys. Rev. B **36**, 7 (1987).
[12] M. Wilke, R. Zimny, and H. Winter, Nucl. Instrum. Methods Phys. Res. B **100**, 396 (1995).
[13] H. Winter, C. Auth, A. Mertens, A. Kirste, and M. J. Steiner, Europhys. Lett. **41**, 437 (1998).
[14] A. Närmann, R. Monreal, P. M. Echenique, F. Flores, W. Heiland, and S. Schubert, Phys. Rev. Lett. **64**, 1601 (1990).
[15] R. H. Ritchie and J. R. Manson, Phys. Rev. B **49**, 4881 (1994).
[16] A. Mertens and H. Winter, Phys. Rev. Lett. **85**, 2825 (2000).
[17] C. Kittel, *Introduction to Solid State Physics*, 6th ed. (Wiley, New York, 1986).
[18] P. M. Echenique and A. Howie, Ultramicroscopy **16**, 269 (1985).
[19] A. G. Borisov, A. Mertens, H. Winter, and A. K. Kazansky, Phys. Rev. Lett. **83**, 5378 (1999).
[20] R. Pfandzelter, A. Mertens, and H. Winter, Phys. Lett. A **290**, 145 (2001).
[21] E. S. Mashkova and V. A. Molchanov, *Medium-energy Ion Reflection from Solids*, Modern Problems in Condensed Matter Sciences Vol. 11 (North-Holland, Amsterdam, 1985).
[22] T. Hecht, C. Auth, A. G. Borisov, and H. Winter, Phys. Lett. A **220**, 102 (1996).
[23] C. Auth and H. Winter, Nucl. Instrum. Methods Phys. Res. B **93**, 123 (1994).
[24] P. Varga and U. Diebold, in *Low Energy Ion-Surface Interactions*, edited by J. W. Rabalais (Wiley, New York, 1994), p. 355.
[25] H. Winter, Prog. Surf. Sci. **63**, 177 (2000).
[26] H. Winter, Phys. Rep. (to be published).
[27] R. Pfandzelter, Phys. Rev. B **57**, 15 496 (1998).
[28] D. A. Dahl, J. E. Delmore, and A. D. Appelhans, Rev. Sci. Instrum. **61**, 607 (1990).
[29] P. Roncin, J. Vilette, J. P. Atanas, and H. Khemliche, Phys. Rev. Lett. **83**, 864 (1999).
[30] A. Mertens, K. Maass, S. Lederer, H. Winter, H. Eder, J. Stöckl, H. P. Winter, F. Aumayr, J. Viefhaus, and U. Becker, Nucl. Instrum. Methods Phys. Res. B **182**, 23 (2001).
[31] D. J. O'Connor and J. P. Biersack, Nucl. Instrum. Methods Phys. Res. B **15**, 14 (1986).
[32] H. M. Evjen, Phys. Rev. **39**, 675 (1932).
[33] R. W. G. Wyckoff, *Crystal Structures*, 2nd ed. (Wiley, New York, 1965), Vol. I, p. 88.
[34] S. Huzinaga, Technical report, 1971 (unpublished).
[35] J. Wasilewski, V. Staemmler, and S. Koch, Phys. Rev. A **38**, 1289 (1988).
[36] S. F. Boys and F. Bernardi, Mol. Phys. **19**, 553 (1970).
[37] G. E. Laramore and A. C. Switendick, Phys. Rev. B **7**, 3615 (1973).
[38] K. H. Rieder, Surf. Sci. **118**, 57 (1982).
[39] N. Garcia, Phys. Rev. Lett. **37**, 912 (1976).
[40] E. Meyer, H. Heinzelmann, D. Brodbeck, G. Overney, R. Overney, L. Howald, H. Hug, T. Jung, H.-R. Hidber, and H.-J. Güntherodt, J. Vac. Sci. Technol. B **9**, 1329 (1991).
[41] G. Benedek and N. Garcia, Surf. Sci. **103**, L143 (1981).
[42] R. J. Glauber, Phys. Rev. **98**, 1692 (1955).
[43] M. C. Desjonquères and D. Spanjaard, *Concepts in Surface Physics* (Springer, Berlin, 1993), p. 135.
[44] H. Hoinkes, H. Nahr, and H. Wilsch, Surf. Sci. **46**, 129 (1974).
[45] J. R. Bledsoe and S. S. Fisher, Surf. Sci. **46**, 129 (1974).
[46] G. Armand, L. Lapujoulade, and Y. Lejay, Surf. Sci. **63**, 143 (1977).